Characterization of Interfaces in Core−Shell Polymers by Advanced Solid-State NMR Methods

Katharina Landfester, Christine Boeffel, Morand Lambla,† and Hans W. Spiess*

Max-Planck-Institut für Polymerforschung, Ackermannweg 10, Postfach 3148, D-55021 Mainz, Germany, and Ecole d'Application des Hauts Polymères/CNRS, 4 rue Boussingault, Strasbourg, France

Received January 23, 1996; Revised Manuscript Received May 14, 1996[⊗]

ABSTRACT: Core−shell latexes based on poly(butyl acrylate) and poly(methyl methacrylate) and latexes of poly(butyl acrylate) and polystyrene were synthesized at high and low temperatures. In both cases the shell content was 33% in weight. Transmission electron microscopy and advanced NMR techniques have been used to investigate the structure of the system, and particular emphasis was put on the characterization of the interface between the two components. This interface can sensitively be analyzed using ^{1}H spin-diffusion techniques. Dynamic gradients at the interface are detected with varying filter strengths of the dipolar filter selecting mobile components and 2D wideline separation (WISE) NMR spectra in which structural and dynamic information are correlated. These experiments show distinct differences in the interface structure of systems synthesized at different temperatures and those with poly(methyl methacrylate) or polystyrene in the shell, respectively.

Introduction

Emulsion polymerization is a well-known technique for preparing latex polymers with defined structures. Depending on the polymerization parameters and conditions, the reaction can selectively yield a variety of particles with different morphologies,[1−4] e.g. core−shell, sandwich structures, hemispheres, and raspberry- or confetti-like structures.

The synthesis of core−shell latexes usually does not lead to an ideal core−shell morphology with a complete phase separation.[5] Figure 1 displays possible substructures of such core−shell latexes with different interfaces. These interfaces consist of mixed phases which are composed of the core and the shell component. Depending on the compatibility of the two polymers and the reaction conditions, the components in the interface can be mixed on a molecular level with a continuous concentration gradient or microdomains can be formed.

The morphology of the entire particle and the interface between the two components in core−shell polymers can sensitively change the macroscopic properties of materials over a wide range. Therefore, the investigation of the particle morphology is an important task for further applications of core−shell systems such as paints, adhesives, coatings, or impact resistant plastics. The microscopic structure is usually characterized by transmission electron microscopy (TEM),[6] and X-ray,[7] light, or neutron scattering.[8] A direct picture of the structure can be obtained by TEM. The limitation of this method lies in the fact that often a distinction of different phases is only possible after staining the sample. Moreover, with standard resolution of about 10 nm it is difficult to characterize substructures in the particles. The scattering methods are very sensitive for samples with periodic structures. By neutron scattering detailed information about the interface between two films can be obtained, but sufficient contrast in such measurements can only be achieved using partially deuterated samples.

As far as NMR is concerned, it is possible to detect fractions with different mobilities by NMR-relaxation time measurements.[9] Moreover, advanced solid-state NMR methods have been developed for the characterization of heterogeneities in polymers and polymer blends.[10,11] They allow one to characterize the morphology including the substructure in the interface and its thickness.

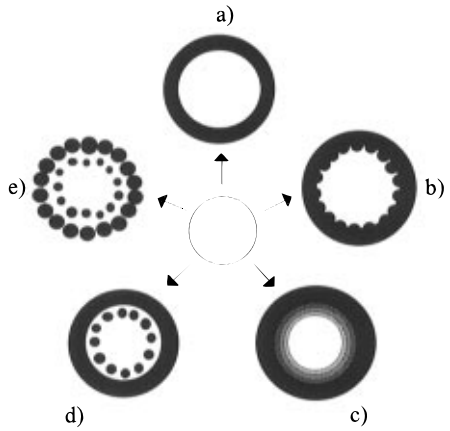

Figure 1. Morphologies deviating from the (a) ideal core−shell: (b) interface with a wavy structure; (c) interface with a gradient of both components; (d) interface with microdomains; (e) microdomains in the interface and an island structure as shell.

In this paper core−shell latexes based on poly(butyl acrylate) (PBuA) and poly(methyl methacrylate) (PMMA) or polystyrene (PS) are studied. The PMMA and the PS are chosen because of their different hydrophilicities from PBuA. Because the PMMA shell is more hydrophilic than PBuA, a particle with core−shell structure is expected. In the case of PBuA/PS the PS is more hydrophobic and should not form a shell around the PBuA core. The particles were synthesized in a two-step emulsion polymerization process with the synthesis of the core in the first step. The second step consisted of the shell polymerization which was performed at high and low temperatures. The particle sizes were determined by TEM and dynamic light scattering (DLS). Detailed information about the morphology including the substructure of the interface was obtained using advanced solid-state NMR methods. It is shown that

† Ecole d'Application des Hauts Polymères/CNRS.

⊗ Abstract published in *Advance ACS Abstracts,* August 1, 1996.

S0024-9297(96)00095-2 CCC: $12.00

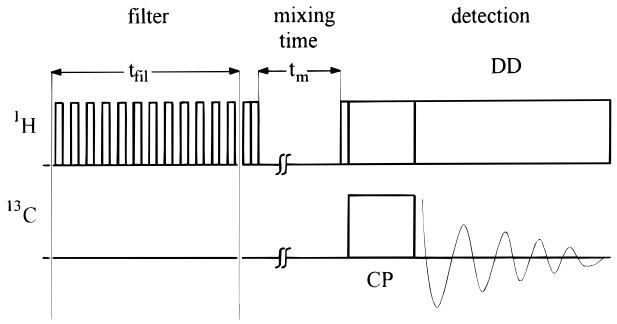

Figure 2. Pulse sequence of the spin-diffusion experiment. In the first step 12 ^{1}H 90° pulses for selecting one component are necessary; the time t_{fil} can be changed by varying the delay between the pulses or by reapplying the multipulse sequence several times. In the mixing time t_m the spin diffusion takes place. The resulting magnetization is detected in ^{1}H spectra or after cross-polarization (CP) in ^{13}C spectra (DD = dipolar decoupling; t_{fil} = filter time; t_m = mixing time).

the NMR methods are applicable not only for the characterization of core−shell particles but also for the characterization of particles with a different structure.

Experimental Section

Synthesis. A set of poly(butyl acrylate)/poly(methyl methacrylate) (PBuA/PMMA) core−shell latexes and poly(butyl acrylate)/polystyrene (PBuA/PS) latexes was synthesized in a semicontinuous process of emulsion polymerization performed in a 1 L reactor.[12]

For the synthesis of the PBuA core with a size of about 350 nm, 270 mL water, 3.0 mL of a 0.5% solution of sodium dodecylbenzenesulfonate as detergent, 13 mL of a 1.57% solution of $(NH_4)_2S_2O_8$ as a water soluble initiator, and 15.0 g of butyl acrylate were put forward in the main reactor. After a nucleation time of 2 h from reactor I a pre-emulsion composed of 355 g of butyl acrylate (with 0.25% of the cross-linking agent ethyleneglycol dimethacrylate (EGDMA)) and 55 mL of a 3.73% solution of sodium dodecylbenzenesulfonate and from reactor II 55 mL of a 1.57% solution of initiator $(NH_4)_2S_2O_8$ were pumped into the main reactor with addition rates of 1.7 and 0.23 mL min^{-1}, respectively. The reaction temperature was 72 °C, the stirring speed was 250 min^{-1}. After completion of the addition the temperature was raised to 85 °C for 5 h to reach high conversion and to dissociate the remaining initiator.

The polymerization of the PMMA shell was performed at different temperatures, namely at 20 and 72 °C, referred to in the following as low- and high-temperature processes, respectively. For the latexes with a shell content of 33 wt % synthesized at the low temperature (20 °C) a pre-emulsion of 134 g of methyl methacrylate (33 wt %), 62 mL of a 3.73% solution of sodium dodecylbenzenesulfonate, 10 mL of a 1.57% solution of $(NH_4)_2S_2O_8$, and 1 g of $Na_2S_2O_5$ as the redox system was added with a rate of 0.2 mL min^{-1} to 600 g of the core latex (44.7 wt % solid content) in the main reactor. To guarantee the decomposition of the initiator even at the low temperature, the redox system of $(NH_4)_2S_2O_8$ and $Na_2S_2O_5$ was used as the initiator. The reaction time after the addition was 24 h. For the high-temperature process the same pre-emulsion without $Na_2S_2O_5$ was added with an addition rate of 3.4 mL min^{-1}. The temperature during the addition was 72 °C and was raised to 85 °C after the addition. The reaction time after addition was about 4 h. Because of the uniform particle size determined by DLS (see below), a second nucleation to form pure PMMA particles can be excluded. The PBuA/PS latexes with 50 wt % shell content were synthesized under the same conditions with a preemulsion of higher composition.

Table 1 gives an overview about the particles and abbreviations used in the following. CS is the abbreviation for core−shell; LT and HT are for low temperature and high temperature, respectively. The number 400 indicates the size of the latexes.

Transmission Electron Microscopy (TEM). The characterization by TEM was performed with a Zeiss EM 902 with an integrated electron energy loss spectrometer. The acceleration voltage was 80 keV. The latex was diluted to a solid content of 0.40 wt %, and several drops of the diluted emulsion were put on an object slide. After evaporation of the water the sample was shadowed with platinum/carbon at an angle of 20°. Subsequently, a carbon supporting film was evaporated and the sample was floated off onto water and transferred to specimen supporting grids as usual. The carbon evaporation was performed in some cases while rotating the sample.

Table 1. Characterization of the Different Particles Synthesized

latex	reaction temp (°C)	diameter by DLS (nm)	content PMMA or PS (% by wt)
CSHT-400	72	385	33
CSLT-400	20	340	33
PBuA/PS	72	420	50

Light Scattering. The particle sizes were determined by a Malvern Autosizer II C.

NMR. ^{1}H and ^{13}C NMR spectra were recorded on a Bruker MSL-300 NMR spectrometer equipped with a standard Bruker MAS probe head. All samples were spun at frequencies of 3 kHz. The 90° pulse lengths were in the range of 3.5−4.0 ^{13}C magnetization; dipolar broadband decoupling (DD) was used to eliminate heteronuclear ^{13}C−^{1}H dipolar coupling. The ^{1}H spin-diffusion experiments were carried out with selection of the soft component PBuA using the dipolar filter.[13] As indicated in Figure 2 one filter cycle consists of a pulse sequence of 12 ^{1}H 90° pulses separated by a delay time t_d of 10 μs and can be repeated 1−20 times.

Typically, 100−200 scans for the ^{1}H spectra and 3000−5000 scans for the ^{13}C spectra were accumulated with a repetition time of 2 s. The measuring time for a ^{1}H spectrum was about 5 min, for a ^{13}C spectrum up to 3 h. All chemical shifts are given relative to tetramethylsilane (TMS) as the external reference.

Results and Discussion

Particle Size. The core−shell particles are typically analyzed with techniques such as dynamic light scattering (DLS) and transmission electron microscopy. The absolute size of hydrodynamic diameter d_n of the high-temperature latex obtained by DLS was determined from the diffusion coefficient D_z to be 385 nm, while the size of the low-temperature latex was determined to be 340 nm. The PBuA/PS particles have a diameter of 420 nm. The standard deviation was obtained as an inverse z-average $\langle d_n^{-1}\rangle_z^{-1}$ from a cumulant expansion of the electric field autocorrelation function. The relative width of the distribution as defined by the second cumulant was on the order of less than 10%. DLS investigations also show that the MMA does not diffuse as monomer into the core but as oligomer. An addition of this monomer to the PBuA-core latex does not change the particle size during 1 h. When initiator is added to this dispersion, the particle is built up.

Transmission Electron Microscopy. The global structure of the particles can be well detected by transmission electron microscopy (TEM). Figure 3a shows representative particles of the low-temperature latex CSLT-400 with a uniform size. The detail structure of one particle is shown in Figure 3b for the low-temperature latex with a shell content of 33 wt %. The photograph shows a core−shell morphology with a complete shell. Since PMMA is decomposed by the electron irradiation, the particle is coated with carbon or with platinum/carbon. Before the irradiation the shell of the particle is intact and the particles cannot form a film; during the electron irradiation the shell of PMMA is partially decomposed and the carbon slumps down to a ring surrounding the remaining particle. On

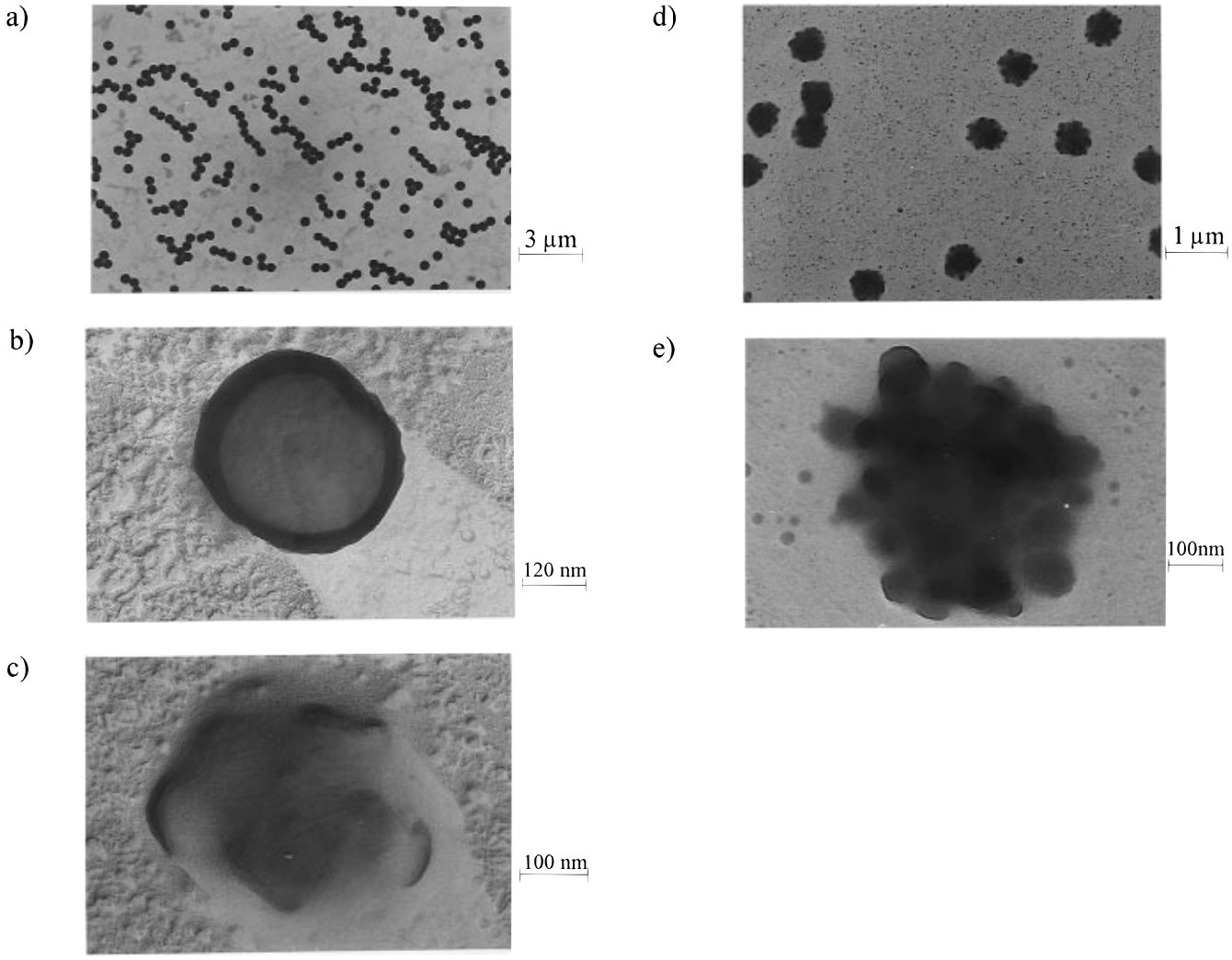

Figure 3. TEM photographs: (a) several particles of CSLT-400; (b) a representative particle for the characterization of the core−shell structure of CSLT-400; (c) a particle of CSHT-400 coated for contrast with platinum and carbon. The shell content is 33% by weight. Note that the shell in the high-temperature latex is incomplete, whereas the low-temperature latex has a thin complete shell. (c) and (d) show particles with different magnifications of the PBuA/PS latex coated with carbon. TEM detects only the global structure; a substructure is not visible.

the contrary a high-temperature latex of PBuA/PMMA with the same shell content of 33 wt % has only very thin shells which are partially incomplete (Figure 3c). Because of the low T_g of PBuA (−45 °C) the particles begin to form a film even during the preparation. In the photograph the particle is deformed. If the same latex is stained with phosphotungstic acid, the latex is stabilized and microdomains can be detected on the surface.[14] This indicates that the fraction of PMMA that diffuses into the core during the reaction is higher for the high-temperature than for the low-temperature latex. For all cases the shells are thinner than calculated from the molar mass ratio of the components introduced during the synthesis. Figure 3d,e shows TEM photographs of a PBuA/PS latex with different magnification. The particles are synthesized at high temperatures. In this case PS does not build a shell around the core, but it forms microdomains with a diameter of about 15 nm. Artifacts in the background of the photograph are caused by the preparation. Particles with a confetti-like morphology are built up. Because of the higher hydrophilicity of the PBuA, the PS seems to have the tendency to diffuse into the core to prevent contact with the aqueous phase. It can be shown that the microdomains grow up when the PS content is increased to 50 wt %; new microdomains are not formed. This confetti-like structure is formed at high and low temperatures. Therefore the following characterizations are performed on one high-temperature latex only.

Solid-State NMR Investigations. Evidently, the morphology and the thickness of the interface of the PBuA/PMMA latexes depend on the synthesis conditions and the sizes of the particles. To elucidate the relationship between morphology, interface structure, and preparation conditions, advanced solid-state NMR techniques,[10] involving WISE experiments[15] and spin-diffusion,[16] are used for the characterization of the particles. The core−shell latexes are composed of mobile PBuA with the low T_g of −45 °C and the high-T_g component PMMA (T_g = 120 °C). At the interface a contact region of the two components is built up. This leads to a partial immobilization of the soft component and a mobilization of the rigid component. This gradient of mobility can be characterized by the dipolar filter. The WISE experiment detects the quality of the phase separation. The PMMA mobilized by the PBuA can be quantified by filter experiments with ^{13}C detection. ^{1}H spin diffusion allows the quantification of the immobilized PBuA. This experiment allows also the determination of the thickness of the interface.

WISE Experiments. The 2D WISE (WIdeline SEparation) experiment allows the combination of structural and dynamic information obtained from the isotropic

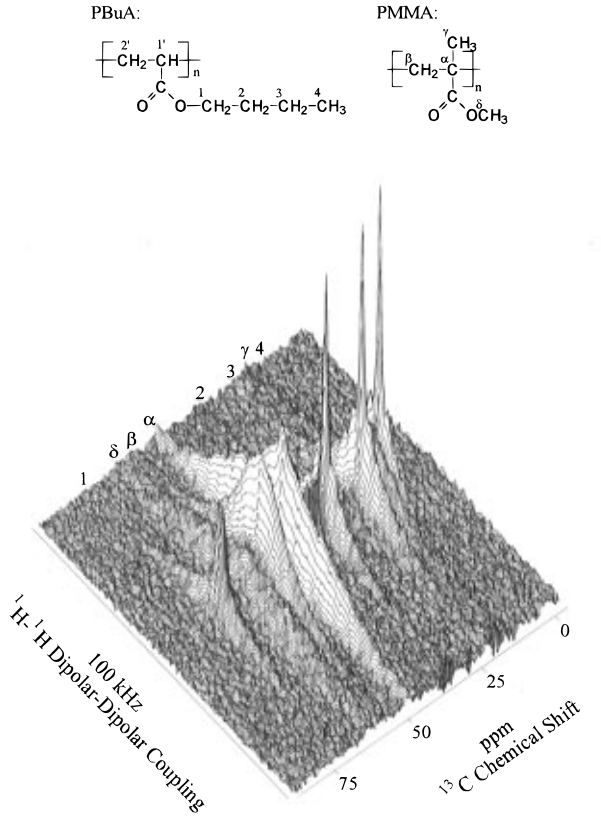

Figure 4. 2D WISE spectrum of the low-temperature latex CSLT-400 with assignment of ^{13}C chemical shifts.

chemical shift in the ^{13}C dimension and the proton line shape in the ^{1}H dimension, respectively. These 2D NMR spectra reveal changes of mobility in different chemical surroundings making use of the ^{1}H NMR line widths. As an example the 2D WISE spectrum of the low-temperature latex CSLT-400 is shown in Figure 4 and selected slices for different systems are plotted in Figure 5.

As expected for PMMA with its T_g well above room temperature, the slices (d and e) in Figure 5 are broadened in the ^{1}H dimension due to the large dipolar couplings. The superposed narrow lines result from mobilized components in the interface. PBuA (slices a and b) also shows a superposition of narrow and broad lines. However, the narrow components are much stronger, indicating higher chain mobility.

Thus, the WISE spectrum reveals the existence of a pure PBuA phase and a pure PMMA phase and a region where the two components are mixed. In the interface the dynamics of both the rigid and the mobile components are different from the respective dynamical behavior in the pure phases.

Therefore, it is interesting to compare WISE spectra for the high- and low-temperature latexes. ^{1}H slices for the C_2 signal of PBuA at 31 ppm are plotted in Figure 5 for the low-temperature latex CSHT-400 (a) and the high-temperature latex CSLT-400 (b). For the latex CSLT-400 the line width of the immobilized component is larger and the intensity of this component is higher than for the latex CSHT-400. This indicates that in the low-temperature latex a larger amount of PBuA is immobilized than in the high-temperature latex. The lines of PMMA for C_α at 45 ppm are shown in Figure 6. The slices are very similar to each other. In both cases a sharp line on the top can be detected, indicating mobilized PMMA.

The WISE spectrum of the PBuA/PS (not shown) indicates more effective phase separation of the two

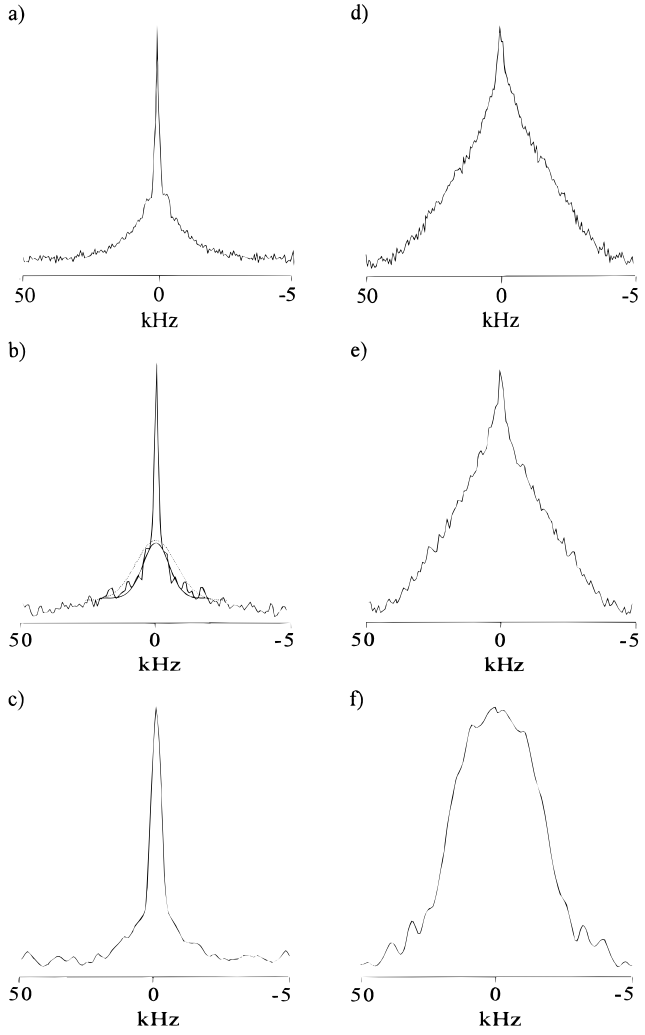

Figure 5. Comparison of ^{1}H line shapes of the PBuA signals (^{13}C chemical shift at 31 ppm) in the WISE spectra plotted for (a) the low-temperature latex CSLT-400 and (b) the high-temperature CSHT-400. The straight line is the Gaussian fit for the line which is smaller compared to the dashed line, indicating the Gaussian fit of the line width of the latex CSLT-400. (c) shows the line shape of PBuA for the PBuA/PS latex. The slices for the PMMA signal at 45 ppm are plotted for (d) the low-temperature latex CSLT-400 and (e) the high-temperature latex CSHT-400. (f) shows the slice of PS at 40 ppm for the PBuA/PS latex.

components. The PS shows very broad lines, as detected from the PS slice at 40 ppm in Figure 5 f, and nearly no narrow component is detected in the PS slice for both high- and low-temperature latexes. The PBuA has narrow lines, but the line width is larger and more homogeneous than in the PBuA/PMMA systems, as shown, e.g., in Figure 5c. In this case the PBuA is slightly immobilized over the whole particle. The direct interface between the two phases must be larger, but the interface region where the two components are mixed is smaller.

Filter Experiments—Quantification of Mobilized PMMA. The dipolar filter using the pulse sequence described above (Figure 4) selects regions with differences in mobility of the components. It is based on the application of multiple pulse homonuclear decoupling.[10] Although this pulse sequence in principle is capable of averaging the dipolar coupling, it is applied here in such a way that only weak dipolar couplings are averaged and the corresponding signals are retained, whereas strong dipolar couplings lead to irreversible decay. If there are two polymers with an ideal phase separation,

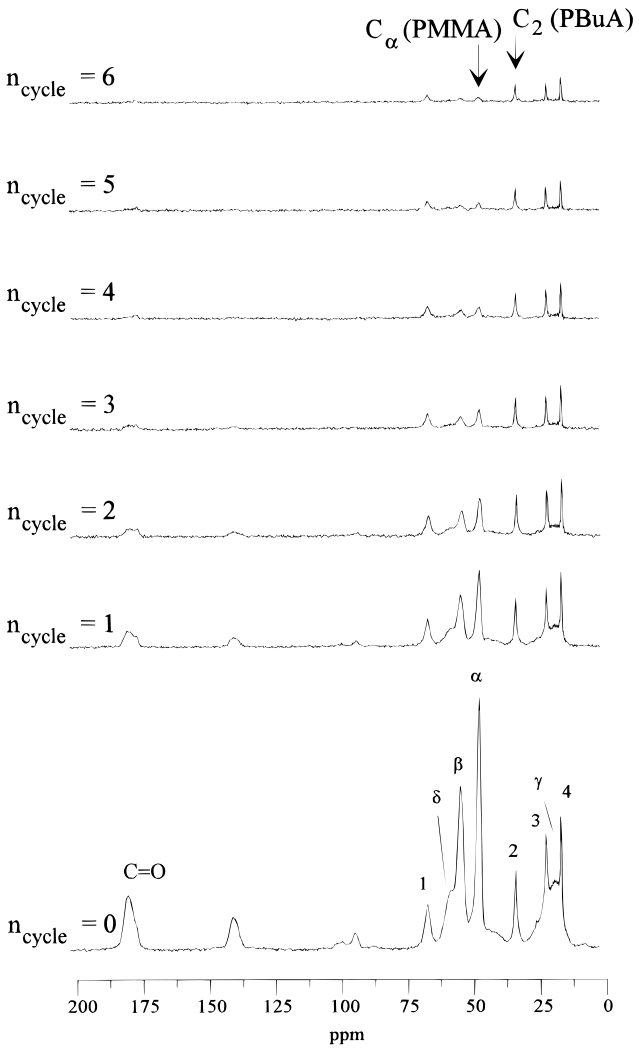

Figure 6. Filter experiments on CSHT-400 with ^{13}C detection. With increasing filter strength the rigid PMMA is suppressed (see arrow at 45 ppm for C_α). Simultaneously immobilized portions of the PBuA are suppressed as visible from the decreasing C_2 signal of PBuA.

only two different components in mobility are found. Generally, there is a region of gradual change in structure and molecular mobility between different phases, the interface. In the case of a mobility gradient dipolar couplings also exhibit a gradual change between the values of the pure phases. Without any filter the whole particle is detected. With increasing filter strength regions with different mobilities can be selected. The strength of the filter can be increased by prolonging the delay time t_d between the pulses or by increasing the number of cycles n_{cycle}. After one filter cycle most of the rigid components with strong dipolar couplings are suppressed. Since the mobility of the soft component is reduced in the interface, this part is also reduced by the dipolar filter. In reverse, the mobilized portion of the rigid components immersed in the core is still detected after applying a weak filter (*e.g.* $n_{cycle} = 1$). The remaining magnetization can be detected in ^1H spectra or after transfer to ^{13}C through cross-polarization in ^{13}C CP/MAS spectra. In the ^1H spectra the mobile component detected as a narrow line can be quantified easily. The evaluation of the rigid component in these spectra is inaccurate because of the broad lines with line widths up to about 50 kHz. The ^{13}C CP/MAS spectra allow an accurate quantification only of the rigid components, but not of the mobile component because the cross-polarization (CP) efficiency of mobile components varies over a wide range.

In filter experiments described in the following the pulse spacing t_d was kept constant at $t_d = 10\ \mu s$. The number of cycles was varied continuously and the magnetization was detected in ^{13}C spectra. NMR spectra without any filtering ($n_{cycle} = 0$) are used as reference for both detection methods.

High-Temperature Latex. In Figure 6 the effect of the dipolar filter on the latex CSHT-400 detected in ^{13}C spectra after magnetization transfer via CP is demonstrated. The ^{13}C spectrum without a filter ($n_{cycles} = 0$) detects the whole particle, as discussed before. With the increasing number of cycles, PMMA and immobilized PBuA are suppressed successively. The PMMA magnetization is evaluated from the signal of C_α at 45 ppm, indicated by the arrow, because there is no overlap with signals of PBuA. The PMMA peaks are only partially eliminated for weak filter strengths. After one filter cycle 70% of the PMMA is suppressed, while 30% are still detected in the spectrum. In view of the differences in CP efficiencies this may be interpreted as indicating that at least 30% of PMMA is mobilized. A total suppression is reached after $n_{cycle} = 5$ where only PBuA signals remain. This demonstrates that this experiment is much more selective than the proton line shapes of Figure 5.

Low-Temperature Latex. The TEM investigations (Figure 3b) allow one to suggest that in the low-temperature latexes a complete shell is already built up at 33% PMMA content. This effect also should be reflected in the substructure of the particles. Indeed, for the low-temperature systems it is more difficult to suppress the PMMA. Because the spectra are similar to those of the high-temperature latex, they are not shown here. For the latex CSLT-400 a number of cycles $n_{cycle} = 7$ is necessary to eliminate the PMMA signal completely. The results of the experiment are shown in Figure 7a. The intensity of the C_α signal is plotted versus the number of filter cycles. The first value without any filter is scaled to 1.0. After one filter cycle 36.8% of the PMMA compared to 30.4% for the high-temperature latex with the same shell content can still be detected.

Comparison of High- and Low-Temperature Latexes. For the low-temperature latex the amount of detected PMMA at weaker filters up to $n_{cycle} = 6$ is always higher than for the high-temperature latexes, as shown in Figure 7b. This indicates a higher mobility of the PMMA in the interface which results if the components are mixed on a molecular length scale.

Thus, in the case of the low-temperature latex an interface with a continuous concentration gradient is expected, as depicted schematically in Figure 1c. The interfacial region of the high-temperature latexes must be different. In spin-diffusion experiments (see below) parts of the PMMA are reached after very short diffusion times. In addition, the shell size is thinner than calculated from the molar mass ratio, while the contact area between the two components must be smaller, resulting from the comparison of the filter experiments. From these findings we conclude that the interface in the high-temperature latex is built up of microdomains. It should be noted that two different kinds of interfaces are present in the particle. As depicted in Figure 7d, there is an extended region between the pure phases with substructures of the rigid component in the mobile one. The gradient region in the high-temperature latex with microdomains is smaller than in the low-temperature latex because of the interfacial region. In addition, the shell as well as each microdomain have

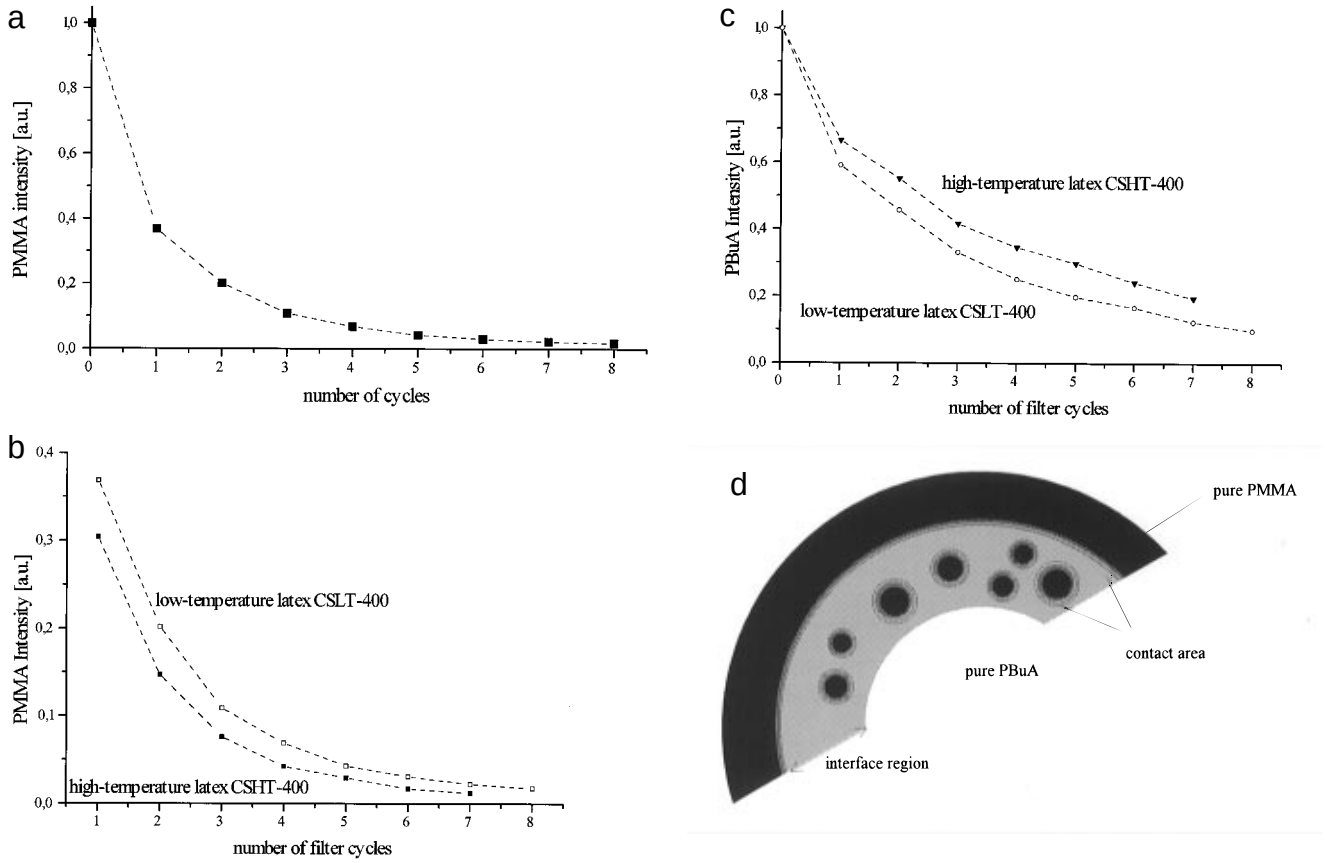

Figure 7. (a) Filter experiment for the low-temperature latex CSLT-400 with ^{13}C detection. The PMMA intensity of the C_α signal is plotted versus the number of filter cycles. The intensity of the first spectrum without any filter is scaled to 1. After one filter cycle 36.8% of PMMA can still be detected as mobilized PMMA. A number of cycles $n_{cycle} = 7$ is necessary to eliminate the entire PMMA. (b) Comparison of the results of the filter experiments with ^{13}C detection for the high- and low-temperature latexes. The PMMA intensity of the C_α signal is plotted versus the number of filter cycles. Note that in the high-temperature latex, contents of mobilized PMMA smaller than in the low-temperature latex are detected for all filter strengths. Note the different scale from (a) to clarify the difference between both latexes. The first value for $n_{cycle} = 0$ is 1, respectively. (c) The PBuA intensity is plotted versus the number of filter cycles. Note that in the high-temperature latex a content of mobile PBuA higher than in the low-temperature latex is detected for all filter strengths. Because of changes in the CP efficiency the PBuA curves cannot be evaluated qualitatively. (d) Both the shell and the substructures have interfacial regions with concentration gradients.

interfacial regions with concentration gradients as discussed for the low-temperature latex.

A second indication for the different interface structures results from the finding that more of the magnetization of PBuA is suppressed in the low-temperature latex CSLT-400 than in the high-temperature latex (Figure 7c). The filter experiments imply that the PBuA in the low-temperature latex is more immobilized, which is expected for a mixing on a molecular level, in contrast to a microdomain formation.

The conclusions reached so far are confirmed by other observations, e.g. the CP efficiency of the two components. In the ^{13}C CP/MAS spectrum of the pure PBuA-core latex the scaled intensity of the PBuA signals is smaller than in the spectra of the core−shell latexes. Comparison of all samples investigated shows that the low-temperature latexes always have higher CP efficiencies than the high-temperature latexes. Therefore, a portion of PBuA in the low-temperature latexes is more immobilized than in the high-temperature latexes. The corresponding ^{13}C one-pulse spectra also show a decrease in the intensity of the PBuA signals for the low-temperature latexes and thus confirm the results of the cross-polarization spectra.

PBuA/PS Latexes. In the case of PMMA a shell is built up around the core with an interfacial region between both phases. The more hydrophobic PS does not build up a shell but only remains inside the core, as determined by TEM (Figure 3e). Even if there is not a core−shell structure, the NMR data allow one to characterize the substructure in the particle. The filter experiments give information of the mobilized portion of PS in the interfacial region around each PS domain; the spin diffusion data (see below) allow one to localize the domains. The filter experiment of the PBuA/PS latex with ^1H detection exhibits a slow decay of the PBuA which indicates its high mobility. This decrease of the mobile components corresponds to the detected magnetization of PBuA in the experiment with ^{13}C detection. In this case a change of cross-polarization efficiency is not observed, which indicates the absence of an extended interface for these systems. The magnetization of PS in the filter experiment with ^{13}C detection decreases very fast and is totally suppressed already after four cycles of the dipolar filter (Figure 8). Therefore, only a small portion of PS is mobilized in an interface and an effective phase separation can be proposed for the PBuA/PS latexes from the filter experiments.

Spin-Diffusion Experiments−Quantification of Immobilized PBuA and Determination of the Interface Thickness. The spin-diffusion experiments allow the characterization of heterogeneities on the length scale of one monomer unit up to 150 nm.[10] A typical ^1H spin-diffusion experiment consists of three steps: first, the proton magnetization of one component is selected by a suitable filter to generate a nonequilibrium distribution of proton magnetization; second, ^1H

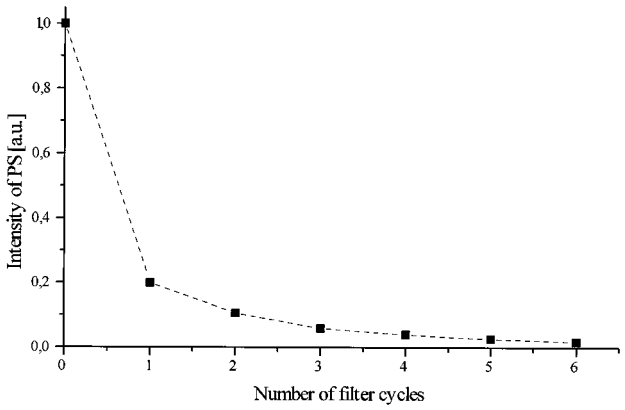

Figure 8. Filter experiment of the PBuA/PS latex. The PS intensity of the C_α signal at 40 ppm is plotted versus the number of filter cycles. The detected PS magnetization decreases with increasing filter strength and is totally suppressed after four cycles of the dipolar filter.

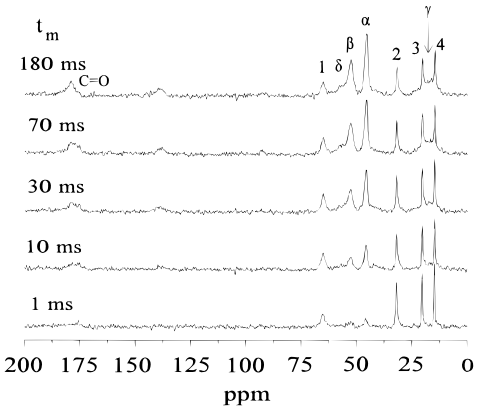

Figure 9. ^{1}H spin-diffusion experiment of the latex CSHT-400 with ^{13}C detection. Using a filter strength of $n_{cycle} = 6$ initially only PBuA is detected ($t_m = 1$ ms). Due to spin diffusion the PMMA signal rises with increasing mixing time and the equilibrium distribution of magnetization is reached after 180 ms.

spin diffusion, i.e. a spatial diffusion of nuclear magnetization without material transfer, occurs during a mixing time t_m which is varied systematically; third, the resulting distribution of proton magnetization after the mixing time is detected in a ^{1}H spectrum or after cross-polarization in a ^{13}C spectrum.

High-Temperature Latex. Because the particle size in these experiments is as large as 400 nm, the spin-diffusion technique is not sensitive to the entire structure.[14] This is due to the low spin-diffusion constant of the mobile component[17] and the spin−lattice relaxation time T_1 in the range of 1000 ms. However, in the case of the PBuA/PMMA latexes spin-diffusion data provide a sensitive measure of the thickness and the structure of the interface.[18]

In Figure 9 the results of the ^{1}H spin diffusion with ^{13}C detection of the high-temperature latex CSHT-400 are shown.[14] For the quantitative analysis the C_α signal of PMMA at 45 ppm and the C_2 signal of PBuA at 31 ppm can be used because they show no overlap with other signals. Using a strong filter with $n_{cycle} = 7$ after a very short mixing time (1 ms) the magnetization of the PMMA is almost completely suppressed and the PBuA is selected. With increasing mixing time the magnetization of PMMA detected in the ^{13}C spectra increases. The high-temperature latexes show redistribution to equilibrium after 180 ms; compare the spectrum for $t_m = 180$ ms in Figure 9 with that for $n_{cycle} = 0$ in Figure 6. With increasing PMMA magnetization

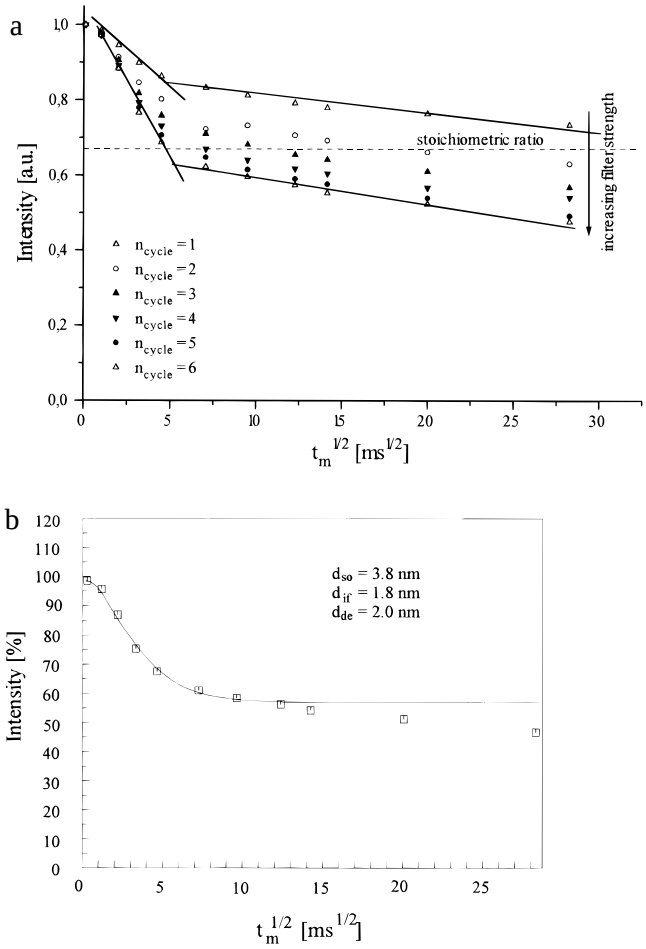

Figure 10. (a) Spin-diffusion experiment for the latex CSHT-400 with ^{1}H detection and varying filter strength. The intensity of the PBuA signal is plotted versus the square root of the mixing time. Note the decrease of the end value with increasing filter strength and the differences in decay at small mixing times, indicating the interface of the particles. (b) Fit for the determination of the interface thickness using the curve with $n_{cycle} = 6$. The parameters were diffusion coefficient of the mobile component 0.1 nm^2 ms^{-1} and diffusion coefficient of the rigid component 0.8 nm^2 ms^{-1}. The thickness of the interface is $d_{so} + 2d_{if} + d_{de} = 9.4$ nm.

the PBuA signal should decrease because the sum of both intensities must be constant during the experiment. As mentioned above, due to the differences of the cross-polarization efficiency in the interface, the signal intensity of the PBuA does not change or even rises during the experiment. The increase of the signal intensity of the PBuA is another sign that a portion of the PBuA which was initially suppressed due to immobilization is now remagnetized by spin diffusion.

In order to quantify the thickness of the interface, ^{1}H spin-diffusion experiments with ^{1}H detection were carried out with varying filter strengths. As an example the results for the high-temperature latex CSHT-400 are shown in Figure 10. The number of cycles was varied between 1 and 6. The initial value is always normalized to 1.0. The signal decay occurs in two steps. At short mixing times the magnetization of PBuA decreases rapidly followed by a slower process at longer mixing times. With increasing filter strength the first decay becomes faster. The final value for mixing times corresponds to the amount of mobile component selected in the experiment. After the weakest filter $n_{cycle} = 1$ a fraction of 73% for the high-temperature latex is observed, which is nearly that expected from the mass ratio of the two polymers PBuA and PMMA. With

increasing filter strength the final values in the spin-diffusion experiment are lower, reaching 48% for $n_{cycle} = 6$ because magnetization of PBuA in the interface is also suppressed. The fast decay at short mixing times detects the thickness of the interface region. The data can be fitted with a one-dimensional diffusion model. In the time of about 100 ms the spin diffusion reaches only the interface as a lamellar structure because of the large diameter of the particle. The simulation yields in a size of about 10 nm for the interface thickness. The long-time behavior cannot be described by the same set of parameters due to the superposition of spin-diffusion processes originating from different structures.

Low-Temperature Latex. The redistribution in the low-temperature latex is similar. For the low-temperature latex the equilibrium is reached very fast (70 ms) in the spin-diffusion experiment with ^{13}C detection. The ^1H spin diffusion was again carried out with varying filter strengths. For the low-temperature latex a decay in two steps was detected as well. The final value of the curve using one filter cycle ($n_{cycle} = 1$) is 67% and corresponds to the mass ratio of the particles. However, it must be mentioned that with weak filters mobilized portions of PMMA are selected as well and detected in the final value besides the PBuA. Therefore, the amount of mobile PBuA is even smaller than 67%. With increasing filter strength the final value decreases. At strong filters the PMMA is totally suppressed and the final value corresponds directly to the selected mobile PBuA.

Comparison of the High- and Low-Temperature Latexes. The difference of the interface revealed from the spin-diffusion experiments for the high- and low-temperature latexes can be explained with different material diffusion lengths of the oligomers during the synthesis. Three effects should be considered: First, at high temperatures the oligomers can diffuse easier than at low temperatures, where the higher viscosity results in a reduced material diffusion coefficient. Therefore, the oligomer chains in the high-temperature latexes can diffuse toward each other and form microdomains. Second, at low temperatures microphase separation of polymerized chains may be hindered due to the lower diffusion coefficient. And third, the χ-parameter may change with temperature, resulting in different compatibilities of the polymers.

When identical filter strengths are compared, the detected proton magnetization of PBuA for the low-temperature latex is always smaller than for the high-temperature latex CSHT-400, as seen in Figure 11 for $n_{cycle} = 6$. This means that the amount of mobile PBuA is smaller for the low-temperature latex than for the high-temperature latex. This indicates that the contact area of PBuA and PMMA is larger for the low-temperature latex. Therefore, as stated before, an interface with a molecular mixing of both components is likely. The fit for the low-temperature latex (shown in Figure 11) results in similar values of 10 nm for the interface.

PBuA/PS Latex. The results of spin-diffusion experiments with ^1H detection also show a two-step decay of decreasing magnetization. However, the first magnetization decay for the PBuA/PS latex is slower than for the high-temperature latexes of PBuA/PMMA. This can be explained with larger microdomains in the core. The final values are always higher (Figure 12), even higher than expected from the mass ratio. A constant end value of magnetization is not reached. In this case the microdomains must be in the outer core region. So a pure core of PBuA may be present with another phase which can be compared with the interface region in the PBuA/PMMA latexes.

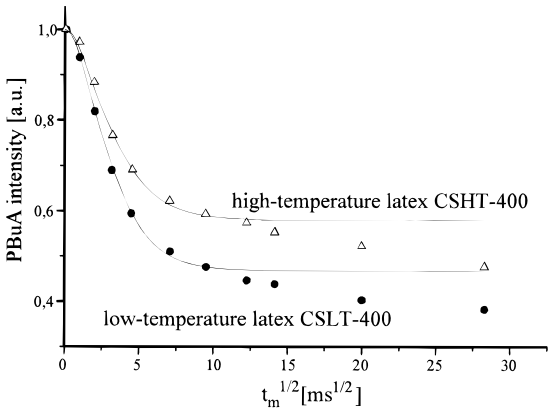

Figure 11. Comparison of the spin-diffusion experiment for the high- and low-temperature latexes CSHT-400 and CSLT-400. The number of filter cycles is $n_{cycle} = 6$. The intensity of PBuA is plotted versus the square root of the mixing time. Note that the values for the magnetization of the low-temperature latex are smaller than for the high-temperature latex, indicating the higher amount of immobilized PBuA in the low-temperature latex.

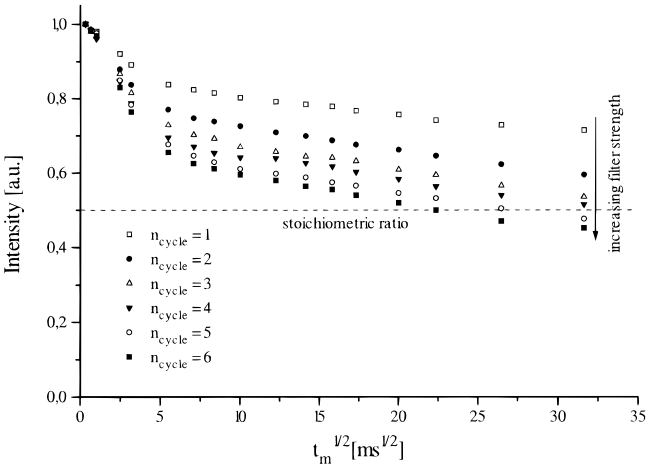

Figure 12. Spin-diffusion experiment with ^1H detection for the PBuA/PS latex with varying filter strength. The intensity of the PBuA signal is plotted versus the square root of the mixing time.

Conclusion

The combination of transmission electron microscopy and advanced solid-state NMR methods allows the characterization of the morphology and the interface structure of PBuA/PMMA and PBuA/PS polymers obtained by a two-step emulsion polymerization. The results of filter-strength, spin-diffusion, and WISE experiments are consistent with the morphologies shown in Figure 13. The PBuA/PMMA latexes have a core−shell morphology with an interface region between the two components which depends on the synthesis conditions. The low-temperature PBuA/PMMA latex consists of core−shell particles with an interface formed by the two components mixed on a molecular level with a continuous concentration gradient of the components. The high-temperature PBuA/PMMA latex forms small microdomains in an interface which is as thick as in the low-temperature latexes. The PBuA/PS latex does not build up a core−shell structure, but the PS forms microdomains in the outer region of the core with an effective phase separation of the components, e.g. a confetti-like structure with little interface. The size of

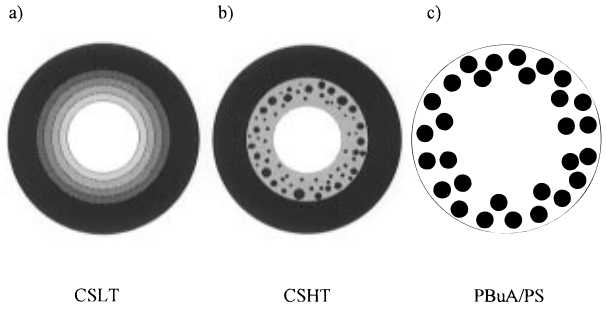

Figure 13. Morphologies predicted from the filter-strength, spin-diffusion, and WISE experiments. (a) The low-temperature latex consists of a core−shell structure with an interface formed by the two components mixed on a molecular level with a continuous concentration gradient. (b) The interface in the high-temperature latexes is built up of microdomains. (c) The PBuA/PS latexes do not form core−shell latexes, but particles with a confetti-like structure.

the microdomains in the system PBuA/PS can be determined by TEM to be 15 nm, while the interface is smaller than 3 nm.

Acknowledgment. Financial support by the Bundesministerium für Wirtschaft (AIF project no. 8858) is gratefully acknowledged. T. Pith and F. Vazquez, Ecole d'Application des Hauts Polymères, Strasbourg, are thanked for helpful discussions in synthesizing the core−shell polymers. It is a pleasure to thank Dr. G. Lieser and G. Weber, MPI für Polymerforschung, Mainz, for their help in the electron microscopic investigations. K.L. thanks the DAAD for a scholarships in Strasbourg (9/1994−2/1995) where the core−shell polymers were synthesized.

References and Notes

(1) Daniel, J. C. *Macromol. Chem., Suppl.* **1985**, *10/11*, 359−390.
(2) Okubo, M.; Katsuta, Y.; Matsumoto, T. *J. Polym. Sci., Polym. Lett. Ed.* **1980**, *18*, 481.
(3) Okubo, M.; *Makromol. Chem., Macromol. Symp.* **1990**, *35/36*, 307.
(4) Okubo, M.; Kanaida, K.; Matsumoto, T. *Colloid Polym. Sci.* **1987**, *265*, 876.
(5) Shen, S.; El-Aasser, M. S.; Dimonie, V. L.; Vanderhoff, J. W.; Sudol, E. D. *J. Polym. Sci., Polym. Chem. Ed.* **1991**, *29*, 857.
(6) Chen, Y. C.; Dimonie, V.; El-Aasser, M. S. *Macromolecules* **1991**, *24*, 3779. Chen, Y. C.; Dimonie, V.; Shaffer, O. L.; El-Aasser, M. S. *Polym. Int.* **1993**, *30*, 185.
(7) Dingenouts, N.; Kim, Y. S.; Ballauff, M. *Colloid Polym. Sci.* **1994**, *272*, 1380.
(8) Hergeth, W.-D.; Bittrich, H.-J.; Eichhorn, F.; Schlenker, S.; Schmutzler, K.; Steinau, U.-J. *Polymer* **1989**, *60*, 1913.
(9) Constantinuous, C.; Tembou Nzudie, D.; Riess, G. *Macromol. Chem., Rapid Commun.* **1993**, *24* (1), 61.
(10) Schmidt-Rohr, K.; Spiess, H. W. *Multidimensional Solid-State NMR and Polymers*; Academic Press: London, 1994.
(11) Clauss, J.; Schmidt-Rohr, K.; Spiess, H. W. *Acta Polym.* **1993**, *44*, 1.
(12) Vázquez, F.; Cartier, H.; Landfester, K.; Hu, G. H.; Pith, T.; Lambla, M. *Polym. Advan. Technol.* **1996**, in press. See also: Landfester, K. Diploma thesis, T. H. Darmstadt, 1993.
(13) Clauss, J.; Schmidt-Rohr, K.; Adam, A.; Boeffel, C.; Spiess, H. W. *Macromolecules* **1992**, *25*, 5208.
(14) Landfester, K.; Boeffel, C.; Lambla, M.; Spiess, H. W. *Macromol. Symp.* **1995**, *92*, 109.
(15) Schmidt-Rohr, K.; Clauss, J.; Spiess, H. W. *Macromolecules* **1992**, *25*, 3273.
(16) Cai, W. Z.; Schmidt-Rohr, K.; Egger, N.; Gerharz, B.; Spiess, H. W. *Polymer* **1993**, *34*, 267.
(17) Spiegel, S.; Schmidt-Rohr, K.; Boeffel, C.; Spiess, H. W. *Polymer* **1993**, *34*, 4566.
(18) Spiegel, S.; Landfester, K.; Lieser, G.; Boeffel, C.; Spiess, H. W.; Eidam, N. *Macromol. Chem. Phys.* **1995**, *196*, 985.

MA960095I